A thermodynamic test of consistency of the data on vapor-liquid equilibrium was not carried out because in our case the equation of Gibbs-Duhem, on which most of these tests are based, is inapplicable (*8*).

Literature Cited

(1) Beilstein IV, 257; E I 417 f; E II 697; E III 547.
(2) Calingert, G., Davis, D. S., *Ind. Eng. Chem.*, **17**, 1287 (1925).
(3) Darzens, J., *C. R. Acad. Sci.*, **208**, 1503 (1939).
(4) Kirk, P. C., Othmer, D. F., *Encycl. Chem. Technol. 2nd Ed.*, **7** (1965).
(5) Strack, B. R., Schwaneverg, M. J., *Ber.*, **86**, 1330 (1933).
(6) Tsugajew, M. P., Sokolow, S. G., *Ber.*, **42**, 56, (1909).
(7) Vilim, O., Hála, E., Pick, J., Fried, V., *Collect. Czech. Chem. Commun.*, **19**, 1330 (1954).
(8) Van Vinkle, "Distillation", McGraw-Hill, New York, N.Y., p 19.
(9) Windows, T. G., Donie, G., Jensen, S., *Ber.*, **54**, 2750 (1921).

Received for review April 22, 1975. Accepted December 15, 1975.

Isothermal Joule–Thomson Coefficients in Mixtures of Methane and Carbon Dioxide

Heng-Joo Ng and Alan E. Mather*
Department of Chemical Engineering, The University of Alberta, Edmonton, Alberta, Canada T6G 2G6

Experimental measurements of the isothermal effect of pressure on enthalpy, $\phi \equiv (\partial H/\partial P)_T$, have been made on two mixtures of $CH_4 + CO_2$ (14.5 and 42.3 mol % CH_4) in the temperature range 273–363 K at pressures up to 137 bar. Comparisons of the results with values calculated from equations of state and using the principle of corresponding states indicate that a modified Benedict–Webb–Rubin equation, utilizing interaction parameters, predicts the effect of pressure on enthalpy within ±2%.

Accurate values of the enthalpy of mixtures over a range of pressures and temperatures are necessary for design of heat exchangers and separation processes. While the enthalpy of many mixtures at low pressures can be calculated from a knowledge of the ideal gas heat capacities, few experimental studies of the effect of pressure on enthalpy have been made. In the usual case, this effect is calculated from P-V-T data together with thermodynamic relations. Accurate direct measurements are desirable for improvements of methods of prediction of the effect of pressure and are useful directly.

In this investigation measurements of the isothermal Joule–Thomson coefficient, ϕ, were made. This property is a direct measure of the effect of pressure on enthalpy:

$$\phi \equiv \left(\frac{\partial H}{\partial P}\right)_T \tag{1}$$

It is related to the adiabatic Joule–Thomson coefficient, μ, by:

$$\phi = -\mu C_p \tag{2}$$

where C_p is the isobaric heat capacity.

Values of ϕ can be obtained from P-V-T data or an equation of state by means of the relation:

$$\phi = V - T\left(\frac{\partial V}{\partial T}\right)_P \tag{3}$$

The value of ϕ at zero pressure is finite and using the virial equation of state can be expressed as:

$$\phi^0 = B - T\left(\frac{dB}{dT}\right) \tag{4}$$

In the present experiments with a finite pressure drop, the values of the enthalpy change determined are converted to values of ϕ by the limiting process

$$\phi = \lim_{P_2 \to P_1}\left[\frac{H_{p2} - H_{p1}}{P_2 - P_1}\right]_{T,x} \tag{5}$$

For comparison with methods of prediction and other results, ϕ values can be integrated to obtain the enthalpy departure

$$(H^0 - H)_T = \Delta H_T = -\int_0^P \phi \, dP \tag{6}$$

Earlier work describing measurements of ϕ have been reviewed by Mather et al. (*13*). Since that time Alkasab et al. (*1*), and Alkasab and Budenholzer (*2*), have described a throttling apparatus utilizing a valve for determination of both ϕ and μ together with results for three mixtures of methane and ethane. Russian workers, Vukalovich et al. (*21, 22, 23*), have also used a throttling valve to measure ϕ for CO_2 and mixtures of $CO_2 + N_2$. Peterson and Wilson (*17*) have also employed a throttling valve for integral measurements of the effect of pressure on enthalpy of CO_2, equimolal $CH_4 + CO_2$ and $CH_4 + C_2H_6 + CO_2$ mixtures. Recently, Pocock and Wormald (*18*) used an adjustable throttle for the measurement of ϕ for N_2 at temperatures from 78 to 298 K at pressures below 6 bar. The results were used to derive second virial coefficients.

This work describes a modified capillary tube throttle, presents data for two mixtures $CH_4 + CO_2$, and compares the experimental results with various methods of prediction.

Experimental Section

A schematic diagram of the apparatus is shown in Figure 1. A Corblin A2CV250 diaphragm compressor is used to recycle the gas under investigation. This compressor operates at constant volumetric throughput and a by-pass under pressure control is used to vary the flow rate through the calorimeter section. A bank of four storage tanks provides additional material for operation up to pressures of 140 bar. The gas passes through buffer tanks to the calorimeter under pressure control. The fluid enters the calorimeter bath, a stainless steel Dewar vessel, and passes through 30 m of copper tubing before entering the throttling calorimeter. Cooling of the bath at the desired operating temperature is provided by water at elevated temperatures and liquid nitrogen at low temperatures. The effect of the coolant is balanced by a temperature controller (Hallikainen Thermotrol) which activates a 500-W heater. After passing through the calorimeter the fluid exits through a manually operated throttling valve which reduces the pressure to about 2 bar. The flow rate is then de-

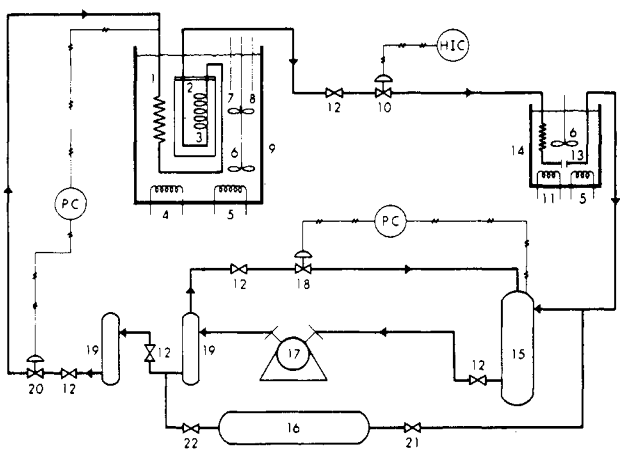

LEGEND

1. Inlet tubing for the Calorimeter
2. Isothermal Calorimeter
3. Capillary Tubing
4. Liquid Nitrogen Cooling
5. Controlled Heat Input
6. Stirrer
7. Platinum Thermometer
8. Sensor for Heat Input Controller
9. Temperature Bath for the Calorimeter
10. Joule Thomson Control Valve
11. Water Cooling
12. Hand Valve
13. Orifice Meter
14. Temperature Bath for the Flow Meter
15. Low Pressure Tank
16. Storage Tank
17. Corblin Diaphragm Compressor
18. By-pass Control Valve
19. High Pressure Tank
20. High Pressure Control Valve
21. Feed Valve
22. Discharge Valve

Figure 1. Flow diagram of the apparatus.

termined by passing the gas through a calibrated orifice meter located in a bath controlled at 30 °C. The gas then returns to the intake of the compressor.

The calorimeter consists of a capillary coil about 3 m in length which causes a pressure drop in the flowing fluid of about 10–15 bar. This pressure drop would usually result in a drop in the temperature of the flowing fluid. However, an insulated Nichrome wire (36 or 40 B&S), which is placed coaxially in the capillary, is used to dissipate electrical energy and to adjust the exit temperature to that of the inlet. Two five-junction copper–constantan thermopiles employed differentially are used to determine the mismatch between the inlet and outlet temperatures. The power from a dc power supply is adjusted manually to achieve temperature equality. The electrical energy supplied is determined by voltage measurements using standard resistors. The pressure drop across the capillary is determined using a variable reluctance pressure transducer which had been calibrated against a dead weight gauge. Efforts were made to minimize heat transfer from the surroundings into the calorimeter. The lead wires for the heater are first brought to an aluminum thermal equalization block before entering the ends of the capillary through Conax glands. A radiation shield completely encloses the capillary coil. The vacuum jacket is evacuated to less than 5 μ to reduce convective heat transfer. Details of the construction of the calorimeter are available in a thesis (*16*).

The inlet temperature of the calorimeter is assumed to be the bath temperature, determined using a platinum resistance thermometer, which had been calibrated by the National Research Council of Canada. The calibration was rechecked by determination of the ice point. The inlet pressure of the calorimeter is measured using a Heise bourdon gauge, which had been calibrated against a Ruska dead-weight gauge. The composition of the flowing gas mixture is determined by means of a gas chromatograph using a thermal conductivity detector and a 1-m column packed with silica gel. The chromatograph was calibrated by the analysis of standard mixtures prepared gravimetrically.

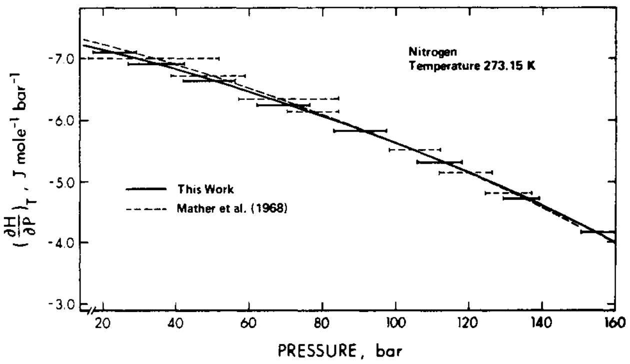

Figure 2. Isothermal data on nitrogen at 273.15 K.

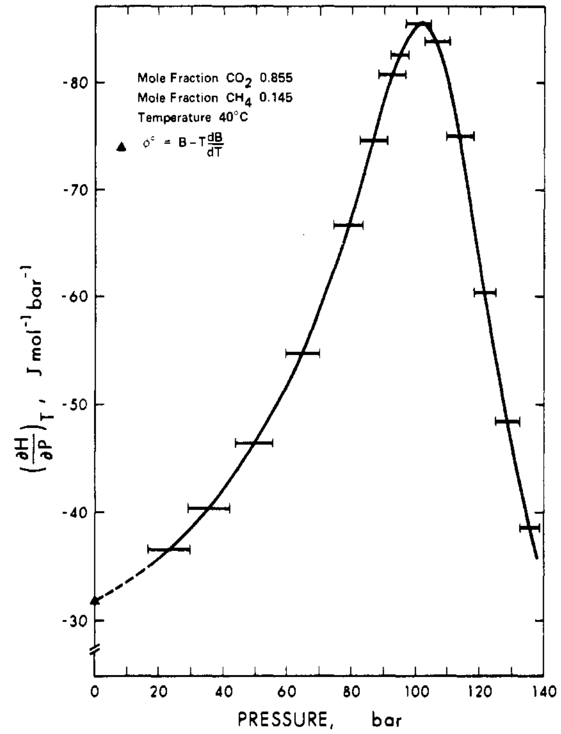

Figure 3. Isothermal throttling coefficient for the 14.5% CH_4 in CO_2 mixture at 40 °C.

Individual measurements of ϕ could be reproduced to ±0.5%. However, the accuracy of the data is not this good. The accuracy is determined by errors in the power input, the flow rate, and the pressure drop. Errors in the measurement of the temperature, composition, and absolute pressure result in uncertainty in the state at which the measurements were made. The accuracy of the results is estimated to be about ±1.5% considering errors in power input (±0.05%), pressure drop (1.0–0.5%), and flow rate (0.5–0.8%), depending upon the pressure level.

Results

Initially, to test the apparatus, the isothermal effect of pressure on the enthalpy of nitrogen was determined at 0 °C at pressures up to 165 bar. The results are shown in Figure 2. The solid lines are the mean value of ϕ over the pressure interval of the experiment. A smooth curve is drawn through the horizontal line segments so that the area underneath the smooth curve is equal to the area under the horizontal lines. The spline fit technique has been used to prepare a smooth curve through these data which contain errors. This method has been described in detail

Table I. Isothermal Throttling Coefficients for 42.3 Mol % Methane in Carbon Dioxide ϕ (J mol^{-1} bar^{-1})

	Temperature, °C			
Pressure (bar)	0	40	60	90
0^a	32.46	24.10	21.30	18.20
10	34.42	24.95	21.92	18.48
20	37.10	25.95	22.58	18.78
30	40.70	27.09	23.28	19.05
40	45.41	28.27	23.95	19.32
50	52.15	29.48	24.60	19.58
60	62.04	30.76	25.20	19.83
70	74.71	32.05	25.76	20.01
80	87.75	33.24	26.27	20.13
90	85.77	34.23	26.69	20.17
100	63.71	34.90	26.95	20.17
110	43.52	34.97	27.00	20.12
120	30.04	34.11	26.76	20.00
130	21.55	32.27	26.17	19.74
137	17.75	31.19	25.53	19.43

^{a} $B - T(dB/dT)$.

Table II. Isothermal Throttling Coefficients in 14.5 Mol % Methane in Carbon Dioxide ϕ (J mol^{-1} bar^{-1})

	Temperature, °C					
Pressure (bar)	0	10	20	40	60	90
0^a	44.23	40.92	36.79	31.91	27.78	23.81
10	49.61	45.64	39.89	33.48	29.18	24.35
20	57.46	51.80	43.82	35.55	30.67	24.97
30	69.86	60.15	48.57	38.28	32.19	25.67
40		73.79	54.82	42.13	33.97	26.54
50		96.73	67.63	46.32	36.04	27.42
60			90.03	51.54	38.37	28.30
70			129.5	58.39	40.92	29.16
80	9.99		241.8	67.48	43.66	30.00
90	7.61	20.90	99.40	78.06	46.53	30.80
100	6.10	14.21	44.51	85.15	49.17	31.48
110	5.02	10.78	25.76	80.53	50.91	31.94
120	3.98	8.43	17.96	63.06	51.07	32.16
130		7.06	14.65	46.30	49.11	32.18
137		6.38	11.54	37.00	46.37	32.11

^{a} $B - T(dB/dT)$.

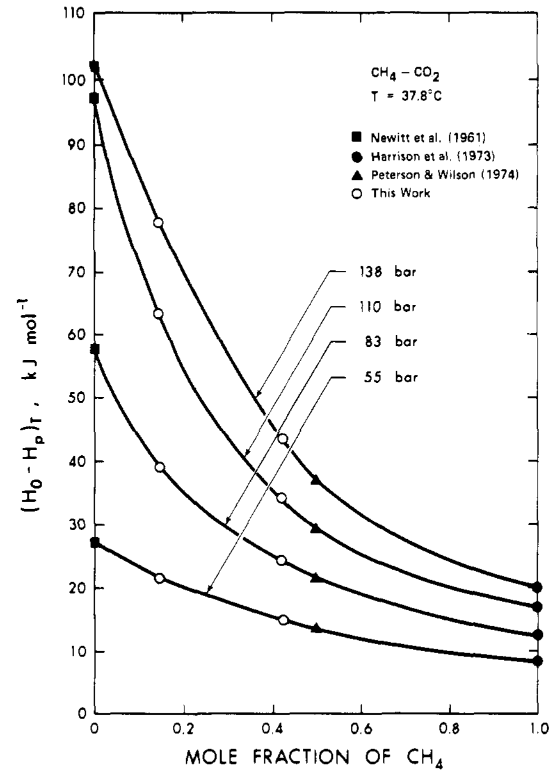

Figure 4. Comparison of enthalpy departures with published data.

by Klaus and Van Ness (*10*). The results at 0 °C agree within ±1% with those of Mather et al. (*12*).

Measurements of the isothermal effect of pressure on enthalpy were made on a mixture containing 42.3 mol % methane in carbon dioxide at 0°, 40°, 60°, and 90° and on a mixture containing 14.5 mol % methane in carbon dioxide at 0°, 10°, 20°, 40°, 60°, and 90 °C. The pressure range of these measurements was from 20 to 140 bar. Figure 3 shows the results for the 14.5% CH_4 mixture at 40 °C. To extend the data to zero pressure, an estimate of ϕ^0 was made using the published second virial coefficients for methane and carbon dioxide, Dymond and Smith (*7*), together with values of B_{12} obtained by Ng (*15*). The estimate is shown as a triangle on Figure 3. Values of ϕ tend towards a uniformly low value at high temperatures, while values near the two-phase envelope are large. The smoothed values of ϕ for these two mixtures are presented in Tables I and II. The extrapolation of the experimental curve to zero pressure allows eq 6 to be used to obtain enthalpy departures from zero pressure to any experimental pressure. Values of the enthalpy departure for the mixtures studied here are compared with the isothermal enthalpy data for an equimolal mixture of $CH_4 + CO_2$ of Peterson and Wilson (*17*) in Figure 4. Enthalpy departures for the pure substances, those of Newitt et al. (*14*), for CO_2 and, those of Harrison et al. (*8*), for CH_4 are also shown. The present results are seen to be in good agreement with Peterson and Wilson (*17*) and are consistent with the departures for the pure components.

Comparison of Methods of Prediction

Two classes of methods of prediction of the enthalpy departure were considered—one based on the principle of corresponding states and the other using an equation of state applicable to mixtures. In the first class, two different correlations were tested—first, that of Yen and Alexander (*25*) which is a revision of the original generalized correlation of Lydersen et al. (*11*), utilizing Kay's rule for the calculation of the pseudocritical pressure, temperature, and critical compressibility factor and second, that of Curl and Pitzer (*6*), again utilizing Kay's rule for calculation of the pseudo-parameters. Two equations of state have been widely used for mixtures—the Benedict-Webb-Rubin and the Redlich-Kwong. Various modifications of these two equations were used to determine enthalpy departures. Three kinds of Benedict-Webb-Rubin equations were tested: (a) the original equation and mixing rules, Benedict et al. (*3*), with values of the constants for CO_2 from Cullen and Kobe (*5*), (b) the Starling and Han (*20*) modification with constants taken from the work of Hopke and Lin (*9*), and, (c) the modified mixing rules of Bishnoi and Robinson (*4*), together with their constants. Two modified Redlich-Kwong equations were used, the Soave (*19*), modification and the Mark V modification due to Wilson (*24*). Both these equations require interaction parameters for the substances present in the mixture and in the calculations, a value of 0.10 was used for the Soave-Redlich-Kwong while a value of 0.105 was part of the Mark V program.

The enthalpy departures calculated by the seven methods of prediction are compared with the experimental departures in

Table III. Enthalpy Departures for 42.3 Mol % CH_4 in CO_2 Compared with Methods of Prediction

T/K	P/bar	$(H^\circ - H)_T$ (J mol^{-1}) This work	Per cent deviation[a]						
			YA (*25*)	CPK (*6*)	SRK (*19*)	MARK V (*24*)	BWR (*3*)	BWRS (*20*)	BWR (B&R) (*4*)
363.15	30	557	−1.1	−7.3	4.3	6.4	4.9	−2.2	−1.1
	70	1340	0.0	−1.2	2.7	4.3	5.4	−2.1	−1.1
	100	1944	1.9	2.4	1.5	2.5	5.9	−2.0	−1.0
	130	2545	3.3	6.2	0.1	0.9	6.1	−2.2	−1.1
	137	2682	3.5	6.5	−0.0	0.5	6.1	−2.2	−1.2
333.15	30	672	−2.6	−6.9	3.2	3.8	6.0	−1.3	1.3
	70	1655	1.0	0.1	2.1	2.3	7.1	−0.8	1.5
	100	2448	4.2	2.4	0.9	0.6	7.9	−0.7	1.6
	130	3252	5.3	4.2	−0.5	−1.2	8.3	−0.9	1.3
	137	3433	5.2	4.0	−1.0	−1.5	8.3	−1.0	1.2
313.15	30	765	−1.8	−3.4	2.9	3.1	8.0	0.4	4.1
	70	1946	4.2	1.3	1.6	1.0	9.1	0.5	3.9
	100	2956	7.6	4.5	0.3	−0.9	10.2	0.5	3.7
	130	3986	6.7	5.6	−1.2	−2.8	10.3	0.0	3.0
	137	4207	6.0	5.4	−1.7	−3.1	10.4	−0.0	2.9
273.15	30	1079	−3.5	3.1	−2.7	−3.6	9.0	0.8	7.2
	70	3244	21.2	11.7	−4.9	−7.4	13.1	−0.2	6.0
	100	5704	4.7	8.8	−4.1	−8.8	17.1	−0.4	3.9
	130	6851	2.9	6.7	−2.5	−5.1	11.3	0.6	3.8
	137	6988	2.9	6.8	−2.6	−4.5	10.7	0.8	3.9
	Absolute average % deviation		4.5	4.9	1.7	3.2	8.8	1.0	2.7

[a] % deviation = [(predicted − experimental)/experimental] × 100.

Table IV. Enthalpy Departures for 14.5 Mol % CH_4 in CO_2 Compared with Methods of Prediction

T/K	P/bar	$(H^\circ - H)_T$ (J mol^{-1}) This work	Per cent deviation[a]						
			YA (*25*)	CPK (*6*)	SRK (*19*)	MARK V (*24*)	BWR (*3*)	BWRS (*20*)	BWR (B&R) (*4*)
363.15	30	735	−12.4	−6.0	4.9	7.6	4.0	−2.9	0.4
	70	1831	−1.4	−0.7	3.4	5.6	4.1	−2.9	0.2
	100	2743	3.6	−0.4	2.0	3.7	4.2	−2.8	0.1
	130	3702	1.8	1.4	0.5	1.8	4.2	−2.8	0.1
	137	3927	1.3	1.6	−0.1	1.3	4.2	−2.9	0.1
333.15	30	894	−8.1	−4.5	3.4	4.6	5.7	−1.3	3.9
	70	2342	4.7	−0.1	2.1	3.0	5.8	−1.6	3.2
	100	3694	7.4	1.3	0.7	1.0	6.3	−1.4	3.0
	130	5210	1.1	1.6	−1.2	−1.4	5.7	−2.0	2.3
	137	5545	0.0	1.9	−1.9	−1.8	5.3	−2.3	2.0
313.15	30	1039	5.7	3.3	1.6	2.1	6.9	−0.4	6.4
	70	2918	11.2	3.0	0.1	0.1	6.8	−1.3	4.9
	100	5095	5.8	5.6	−1.5	−2.7	8.2	−1.4	4.2
	130	7203	3.0	1.5	−2.5	−3.4	5.1	−2.4	2.0
	137	7493	−2.8	1.6	−2.9	−3.0	4.5	−2.3	1.9
293.15	30	1256	−2.6	4.5	−2.6	−2.6	6.2	−1.1	7.2
	70	4209	26.0	33.8	−4.8	−6.1	8.1	−3.6	4.8
	100	8595	−1.1	−0.0	−2.9	−3.9	5.2	−0.8	2.1
	130	9309	3.5	2.0	−1.5	−1.6	2.8	−0.4	2.4
	137	9402	3.9	2.3	−1.7	−1.3	2.5	−0.4	2.3
283.15	30	1478	−4.4	−1.2	−10.2	−10.4	0.1	−7.0	1.7
273.15	30	1529	10.9	7.9	−5.2	−5.8	8.5	−0.5	11.1
	Absolute average deviation		5.6	3.9	2.2	3.4	5.2	2.0	3.0

[a] % deviation = [(predicted − experimental)/experimental] × 100.

Tables III and IV. For the mixtures of methane and carbon dioxide studied, the Starling modification of the B–W–R equation gave the best results, the average absolute deviation being 1.5% with a maximum deviation of −7.0%.

Nomenclature

B = second virial coefficient, cm^3 mol^{-1}

C_p = specific heat capacity at constant pressure, $(\partial H/\partial T)_P$, J mol^{-1} K^{-1}

H = enthalpy, J mol^{-1}

H° = ideal gas enthalpy, J mol^{-1}

P = pressure, bar

T = temperature, K

V = specific volume, cm^3 mol^{-1}

Greek Letters

μ = Joule–Thomson coefficient, $(\partial T/\partial P)_H$, K bar^{-1}

ϕ = isothermal Joule–Thomson coefficient, $(\partial H/\partial P)_T$, J mol^{-1} bar^{-1}

ϕ^0 = zero-pressure isothermal Joule–Thomson coefficient, J mol^{-1} bar^{-1}

Literature Cited

(1) Alkasab, K. A., Shah, J. M., Laverman, R. J., Budenholzer, R. A., *Ind. Eng. Chem. Fundam.*, **10,** 237 (1971).
(2) Alkasab, K. A., Budenholzer, R. A., *Rev. Sci. Instrum.*, **44,** 1561 (1973).
(3) Benedict, M., Webb, G. B., Rubin, L. C., *J. Chem. Phys.*, **8,** 334 (1940); *ibid.*, **10,** 747 (1942).
(4) Bishnoi, P. R., Robinson, D. B., *Can. J. Chem. Eng.*, **50,** 101 (1972).
(5) Cullen, E. J., Kobe, K. A., *AIChE J.*, **1,** 452 (1955).
(6) Curl, R. F., Jr., Pitzer, K. S., *Ind. Eng. Chem.*, **50,** 265 (1958).
(7) Dymond, J. H., Smith, E. B., "The Virial Coefficients of Gases", Clarendon Press, Oxford, 1969.
(8) Harrison, R. H., Moore, R. T., Douslin, D. R., *J. Chem. Eng. Data*, **18,** 131 (1973).
(9) Hopke, S., Lin, C.-J., paper presented at 76th National AIChE Meeting, March 10–13, Tulsa, Okla. 1974.
(10) Klaus, R. L., Van Ness, H. C., *AIChE J.*, **13,** 1132 (1967).
(11) Lydersen, A. L., Greenkorn, R. A., Hougen, O. A., *Univ. Wis. Eng. Exp. Stn. Rep.*, **No. 4** (1955).
(12) Mather, A. E., Katz, D. L., Powers, J. E., *Trans. Faraday Soc.*, **64,** 2939 (1968).
(13) Mather, A. E., Powers, J. E., Katz, D. L., *AIChE J.*, **15,** 111 (1969).
(14) Newitt, D. M., Pai, M. U., Kuloor, N. R., Huggill, J. A., "Thermodynamic Functions of Gases", Vol. 1, F. Din, Ed., 1961, p 102.
(15) Ng, H.-J., M.S. Thesis, University of Alberta, 1971.
(16) Ng, H.-J., Ph.D. Thesis, University of Alberta, 1975.
(17) Peterson, J. M., Wilson, G. M., *Proc. Annu. Conv., Gas Process. Assoc., Tech. Papers*, **53,** 57 (1974).
(18) Pocock, G., Wormald, C. J., *J. Chem. Soc., Faraday Trans. 1*, **71,** 705 (1975).
(19) Soave, G., *Chem. Eng. Sci.*, **27,** 1197 (1972).
(20) Starling, K. E., Han, M. S., *Hydrocarbon Process.*, **51** (5), 129 (1972).
(21) Vukalovich, M. P., Altunin, V. V., Bulle, Kh., Rasskazov, D. S., Ertel, D., *Therm. Eng.*, (*Engl. Trans.*), **16** (11), 99 (1969).
(22) Vukalovich, M. P., Bulle, Kh., Rasskazov, D. S., Ertel, D., *Therm. Eng.* (*Engl. Trans.*), **17** (6), 93 (1970).
(23) Vukalovich, M. P., Bulle, Kh., Ertel, D., *Russ. J. Phys. Chem.*, **46,** 1475 (1972).
(24) Wilson, G. M., DeVaney, W. E., "Mark V Computer Program", available from the Gas Processors Association, Tulsa, Okla.
(25) Yen, L. C., Alexander, R. E., *AIChE J.*, **11,** 334 (1965).

Received for review June 10, 1975. Accepted February 17, 1976.

Solubility of Inorganic Gases in High-Boiling Hydrocarbon Solvents

Kevin K. Tremper and John M. Prausnitz*
Chemical Engineering Department, University of California, Berkeley, California 94720

Low-pressure solubilities have been measured for 19 gas–solvent pairs. Gases and solvents used were: ammonia, nitrogen, carbon monoxide, hydrogen sulfide, hydrogen chloride, carbon dioxide, and sulfur dioxide; *n*-hexadecane, diphenylmethane, bicyclohexyl, and 1-methylnaphthalene. For all pairs, data were obtained in the temperature range 25–200 °C. The accuracy of these data is better than 1%.

Design of chemical processing equipment, especially in the petroleum industry, often requires accurate knowledge of gas solubilities in various solvents over a wide temperature range. However, reliable gas-solubility data are not plentiful and most experimental data have been taken at room temperature. In this work the solubilities of seven gaseous solutes were measured in four high-boiling hydrocarbon solvents in the temperature range 25–200 °C. The experimental apparatus, designed and built by Cukor, is described in detail elsewhere (*4*).

The impetus for this work is twofold. Two previous workers using this solubility apparatus (Cukor (*4, 5, 6*) and Chappelow (*2, 3*)) studied exclusively hydrocarbon solutes. Thus one purpose for this work is to add to the previously reported data the solubilities of several nonhydrocarbon gases. These gases were selected first, because of their industrial importance and second, because of their physical properties. The gases span a range of dipole moment while the hydrocarbon solvents vary in molecular structure and degree of saturation (surface to volume ratio), as shown in Tables II and III. The second purpose of this work is to supply a firm experimental basis from which to develop a widely applicable solubility theory.

Experimental Section

The experimental apparatus and procedure are essentially the same as those described by Cukor (*4, 5*) and Chappelow (*2, 3*). The following is a brief summary of the apparatus and procedure.

Figure 1 shows the experimental apparatus which consists of five sections: (1) a degassing flask, D; (2) an equilibrium cell, enclosed by the dotted box; (3) a reservoir for degassed solvent, E; (4) a precision gas burette, F; and (5) a section for pressure measurement, shown in detail in Figure 2.

The equilibrium cell consists of two volume-calibrated cells; one for solvent A and one for gas B. They are separated by a calibration mark, b. The original cell was modified to allow it to be removed and interchanged with other cells, as discussed in Appendix I.

The experiment begins by degassing the solvent, by alternate freezing and thawing under vacuum. Five repetitions are sufficient to remove the dissolved gases in all cases. The solvent is then transferred to the equilibrium cell and circulated under vacuum for final degassing. The solvent level in A is adjusted to the calibration mark b by draining the excess into the collecting flask E. This flask is then removed and weighed. Since the volume of the liquid section of the cell is known, the initial mass of solvent in the cell is determined from the density at the starting temperature.

The temperature of the bath is raised to the highest desired and the solvent vapor pressure is measured and compared to the literature value. This vapor pressure measurement is a final check on the proper degassing of the solvent. The expanded solvent is again lowered to the calibration mark b. The collecting flask E is again removed and weighed to determine the mass of solvent occupying the solvent cell volume. A known amount of gas is now added to the cell from the precision gas burette F. Equilibrium is attained quickly by circulating the solvent through the vapor space with pump C. Equilibrium is achieved when the pressure in the cell no longer changes at constant temperature, usually in less than 2 h. With the mass of each component known, only the temperature and pressure need be measured to specify the system completely. Once the pressure is measured, the bath is lowered to the next desired temperature. Since the solvent has contracted below the calibration mark b, makeup